One Single Tube Reaction of Aptasensor-Based Magnetic Sensing System for Selectively Fluorescent Detection of VEGF in Plasma

Hwang-Shang Kou , Shao-Tsung Lo , Chun-Chi Wang *

Posted Date: 17 April 2023

doi: 10.20944/preprints202304.0451.v1

Keywords: VEGF; Aptasensor; Streptavidin magnetic bead; Plasma; Hybridization probe

Article

One Single Tube Reaction of Aptasensor-Based Magnetic Sensing System for Selectively Fluorescent Detection of VEGF in Plasma

Hwang-Shang Kou [1], Shao-Tsung Lo [1] and Chun-Chi Wang [1,2,3,*]

[1] School of Pharmacy, College of Pharmacy, Kaohsiung Medical University, Kaohsiung, Taiwan, R.O.C.
[2] Department of Medical Research, Kaohsiung Medical University Hospital, Kaohsiung, Taiwan, R.O.C.
[3] Drug Development and Value Creation Research Center, Kaohsiung Medical University, Kaohsiung, Taiwan, R.O.C.
* Correspondence: chunchi0716@kmu.edu.tw; Tel: 886-7-3121101 ext 2253; Fax: 886-7-3210683

Abstract: In this study, a simple, easy and convenient fluorescent sensing system for detection of vascular endothelial growth factor (VEGF) based on VEGF aptamers, aptamer-complementary fluorescence-labeled probe and streptavidin magnetic beads was developed in only one single tube. The VEGF is the most important biomarker in cancer angiogenesis, and is investigated that serum VEGF level was various according to the different type and course of cancers. Hence, efficient quantification of VEGF is able to improve the accuracy of cancer diagnosis and precision of disease surveillance. In this research, the VEGF aptamer was designed to be able to bind with the VEGF by forming G-quadruplex secondary structures, and then the magnetic beads would capture the none-binding aptamers due to none steric interference, and finally, the fluorescence-labeled probes were hybridized with the aptamers captured by the magnetic beads. Therefore, the fluorescent intensity in the supernatant would specifically reflect the present of VEGF. After an overall optimization, the optimal conditions for detection of VEGF were as followed, KCl, 50 μM; pH 7.0; aptamer, 0.1 μM and magnetic beads, 10 μL (4 μg/μL). The VEGF could be well quantified within a range of 0.2-2.0 ng/ml in plasma, and the calibration curve possessed a good linearity ($y = 1.0391x + 0.5471$, $r = 0.998$). The detection limit (LOD) was calculated to be 0.0445 ng/mL according to the formula ($LOD = 3.3\times\sigma/S$). The specificity of this method was also investigated under the appearance of many other serum proteins, and the data showed the good specificity in this aptasensor-based magnetic sensing system. This strategy provided a simple, sensitive and selective biosensing platform for detection of serum VEGF. Finally, it was expected that this detection technique can be promoted to more clinical applications.

Keywords: VEGF; aptasensor; streptavidin magnetic bead; plasma; hybridization probe

1. Introduction

Under the past decade, magnetic sensing system provided a convenient platform to simplify the process in the development of sensing system, because the magnetic spherical materials could be easily applied to capture the targets and be simply collected by a magnet. Among them, streptavidin and biotin were often utilized in the magnetic sensing system due to their good specific binding [1], and the strong non-covalent binding force between streptavidin and biotin has been also widely used in many detection methods [2–6]. Additionally, the small-scale magnetic beads themselves also have a very high specific surface area, and thus, they have good dispersibility in solutions, and the reaction rate with the target is also very fast. The above advantages make streptavidin-modified magnetic beads widely use and easily operate [7]. However, the magnetic beads could not supply the specific recognizing with the targets. Therefore, several materials for specific binding with the targets were developed, such as traditional antibody, aptamers, molecularly imprinted polymers [8] and so on. Among those, aptamers have the characteristics of low molecular weight, stability, easy modification,

easy synthesis, and itself is not affected by the repeatability, and thus, in most of the current sensing methods, it has gradually replaced the role of the original antibody [9–11]. Aptamers refer to a sequence of about 20-60 nucleotides in length, which can be designed as specific binding with high affinity for different target molecules [12–15]. Under the binding reaction, the aptamers will be flexed into many various secondary structures, such as G-quadruplex which can specifically bind target molecules [16,17]. Therefore, aptamers are often applied in the development of biosensing systems [15,18–20]. In this study, the benefits of the magnetic sensing system and aptamers would be combined to develop an aptasensor-based magnetic sensing system for selectively fluorescent detection of vascular endothelial growth factor, VEGF, in plasma.

VEGF is a key factor in angiogenesis which is the formation and maintenance of blood vessel structures for the physiological functions, and is considered as an important component for the progression of diseases such as cancer and inflammation [21]. When tumor cells are attacked by immune mechanisms and poisonous drugs, they will develop drug resistance through their ability to randomly mutate in large numbers [22–24], making treatment even more difficult. Therefore, the direction of treatment began to shift to blocking tumor development and indirectly inhibiting tumor development, such as blockage of angiogenesis [25–27]. According to clinical literature, vascular endothelial cell growth factor (VEGF) in tumor cells would have a much different blood concentration from normal cells, and the angiogenesis rate of tumor cells is increased to twenty times as many as normal cells [28,29]. In the literature review of meta-analysis in 2007, it was mentioned that the blood concentration of VEGF in breast cancer patients was about 310 pg/mL, which was ten times as high as 30 pg/mL in normal human blood [30]. The blood concentration can be utilized to aid in the diagnosis of cancer types and also to monitor the progression of tumor cells throughout the course of the disease [31–33]. Therefore, rapid and accurate VEGF detection is particularly important.

Until now, a lot of techniques have been developed for detection of VEGF for the current clinical applications, including traditional Western blot [34], immunohistochemistry (IHC) [35], radioimmunoassay (RIA) [36]. At present, the enzyme-linked immunosorbent assay (ELISA) is the most commonly used clinical method for detection of VEGF [37]. In addition, with the recent development of novel biosensing platforms, aptamer-based luminescence detection methods [38–41] were also widely developed. Other methods such as colorimetric system [42], Surface Plasmon techniques [43], Surface Plasmon Resonance imaging (SPRi) [44,45] have also been designed and applied. Among them, most of the methods required expensive testing materials and complex knowledge or operation to process and interpret the data. Therefore, in this study, a method using aptamers, fluorescent probe and simple magnetic bead was developed, which can be rapidly quantified under a fluorescent detector and especially completed in only one single tube. This strategy provided a simple, sensitive and selective biosensing platform for detection of serum VEGF, and it was expected that this detection technique can be severed as a tool for clinical survey, and promoted to more clinical applications in the detection of VEGR.

2. Materials and Methods

2.1. Reagents and materials

VEGF-165 (VEGF, 100 μg/mL) were purchased from Takapouzist Company (Tehran, Iran). VEGF-aptamer and fam-labeled probe were synthesized by MDBio Co., Ltd. (Taiwan), the sequences of those were as shown in Table 1. Streptavidin magnetic beads (4 μg/mL, 1 μm) were purchased from New England Biolabs (Ipswich, MA, USA). Ethanol, 2,2′,2″,2‴-(Ethane-1,2-diyldinitrilo) tetraacetic acid (EDTA) and 2-Amino-2-hydroxymethyl-propane-1,3-diol (TRIS-base) were purchased from J.T.Bake® (Phillipsburg, NJ, USA). The ddH_2O was prepared by Milli-Q® system (Millipore, Bedford, MA, USA). Methanol (analytical grade reagent) and magnesium chloride were purchased from Merck (Merck, Darmstadt, Germany). Potassium chloride were purchased from Scharlau (Barcelona, Spain). Sodium chloride were purchased from PanReac AppliChem ITW reagents (Barcelona, Spain).

Preprints (www.preprints.org) | NOT PEER-REVIEWED | Posted: 17 April 2023 doi:10.20944/preprints202304.0451.v1

Table 1. The sequences of the VEGF aptamer and the fluorescent probes.

Label	Sequence	Length (mer)
VEGF aptamer	5′-TGTGG GGGTG GACGG GCCGG GTAGA TTTTT TTT-3′-Biotin	33
10 mer-probe	5′-CACCC CCACA-3′-FAM	10
15 mer-probe	5′-CCGTC CACCC CCACA-3′-FAM	15
20 mer-probe	5′-CCGGC CCGTC CACCC CCACA-3′-FAM	20

FAM: 6-fluorescein amidite, fluorescent dye.

2.2. The detection of the fluorescence

The measurements of fluorescence were carried out in F-4500 fluorescent spectrometer (Hitachi, Japan). The excitation and emission slit were set at 10 nm and 10 nm, respectively. The scanning speed was set at 1200 nm/min. The fluorescence emission was recorded from 500 to 600 nm and the excitation wavelength was set at 480 nm. All measurements were carried out at room temperature.

The symbol of (F) meant the fluorescent intensity in the presence of different concentrations of the VEGF, and the (F0) meant the fluorescent intensity without VEGF. The final signal for method optimization, calibration curve, specificity and recovery would be expressed as shown in Equation (1).

$$(F - F0)/F0 \quad (1)$$

F: the fluorescent intensity in the presence of VEGF.
F0: the fluorescent intensity without VEGF.

2.3. The one single tube reaction

Firstly, a total of 200 μL solution containing 50 μM KCl and 0.1 μM VEGF-aptamer was prepared in 1X TBSE buffer (10 mM TRIS-Base, 0.05 mM EDTA, 100 mM NaCl and 1 mM $MgCl_2$, pH 7.0). Subsequently, 20 μL solution containing different concentrations of VEGF was added to the solution and incubated at room temperature (25 °C) with shaking for 45 min, and then 10 μL of magnetic beads was added to capture the residual VEGF-aptamer at room temperature (25 °C) with shaking for 1 min. After that, the magnetic beads were collected by a magnet and the supernatant was removed, and then, the magnetic beads were washed with ddH_2O for three times. Finally, a 200 μL of 1X TBSE buffer solution containing 0.01 μM fluorescent probe was added to reconstitute magnetic beads with shaking for 3 min. After precipitating the magnetic beads, the supernatant was collected to measure the fluorescence. The VEGF could be easily quantified through the fluorescent intensity of the supernatant. In the whole procedures, all reactions were completed in one single tube.

2.4. Method validation

In the establishment of calibration curve, different concentrations of VEGF including 0.2, 0.5, 1.5, 2.0 ng/mL spiked into plasma were utilized and proceeded in the one single tube reaction according to the section 2.3. The calibration curve was established by comparison of the fluorescent signal ((F-F0)/F0) (Y axis) with the various concentrations of VEGF in ng/mL (X axis). In this study, the specificity of method was investigated by using the proteins those are also presented in human. In order to show a high degree of specificity of this strategy with using these common proteins, the concentrations of these common proteins were about 20 times higher than those presented in human blood. These proteins contained 20 ng/mL bovine serum albumin (BSA), 20 ng/mL albumin (Albumin), 5×10^{-3} U/mL insulin (Insulin), 2×10^{-3} U/mL mL nitric oxide synthase (NOS). The 2 ng/mL VEGF as control group with using these common proteins was utilized to investigate the specificity according the fluorescent signal ((F-F0)/F0).

 doi:10.20944/preprints202304.0451.v1

2.5. The real plasma samples

The plasma samples were directly analyzed under this technique. Under the optimal conditions for detection of VEGF (KCl, 50 μM; pH 7.0; aptamer, 0.1 μM and magnetic beads, 10 μL (4 ng/μL)), the different concentrations of VEGF were spiked at 0.2, 0.5, and 1.5, 2 ng/mL into plasma to establish the calibration curve of real biological samples. The calibration curve was established by comparison of the fluorescent signal ((F-F0)/F0) (Y axis) with the various concentrations of VEGF in ng/mL (X axis). Additionally, in order to know the quantitative efficiency of the strategy for detection of plasma samples, the two different concentrations of VEGF (0.8 and 1.6 ng/mL) were spiked into the test plasma sample with a real concentration of 0.2 ng/mL, and then the concentrations of VEGF was calibrated according the established regression line in plasma to estimate the recovery of this method in plasma samples.

3. Result and discussion

3.1. The mechanism of one single tube reaction of aptasensor-based magnetic sensing system

In this study, the one single tube reaction of aptasensor-based magnetic sensing system was established for detection of VEGF in plasma. The convenient, simple and fast sensing system was presented that all of the detection could be completed in one single tube. The mechanism was as shown in Figure 1. Firstly, the APTs that have been flexed into a G-quadruplex in an appropriate environment are fully reacted with VEGF at room temperature for 40 minutes to generate a specific complex of non-covalent bonds [46], and the residual APTs would retain the original G-quadruplex configuration in samples without VEGF. Subsequently, the streptavidin-coated magnetic bead (MB) was added into the solution to capture the residual APTs of the original G-quadruplex configuration through its derived biotin group, but the complex of APTs and VEGF would not be captured by the MBs due to the high steric interference. After finishing that, the MBs were collected and purified with an external magnetic field, and the supernatant was removed. Finally, the MBs were washed with 1X TBSE buffer for three times and reconstituted in 1X TBSE buffer, and then the fluorescent probe was added to the MBs whose surface is covered with some APTs. In the presence of VEGF, the residual APTs captured by the MB would be less, resulting in the less amount of fluorescent probes can bind to the MB through the hybridization. Therefore, the fluorescent intensity of the supernatant is higher. On the contrary, in the absence of VEGF, the number of residual APTs on the surface of the MBs would be larger, and more amount of fluorescent probes would be captured by the MBs, while the supernatant has a lower fluorescent intensity. Thus, in this simple design, the VEGF could be specifically quantified through the fluorescent intensity rebound ratio.

Preprints (www.preprints.org) | NOT PEER-REVIEWED | Posted: 17 April 2023 doi:10.20944/preprints202304.0451.v1

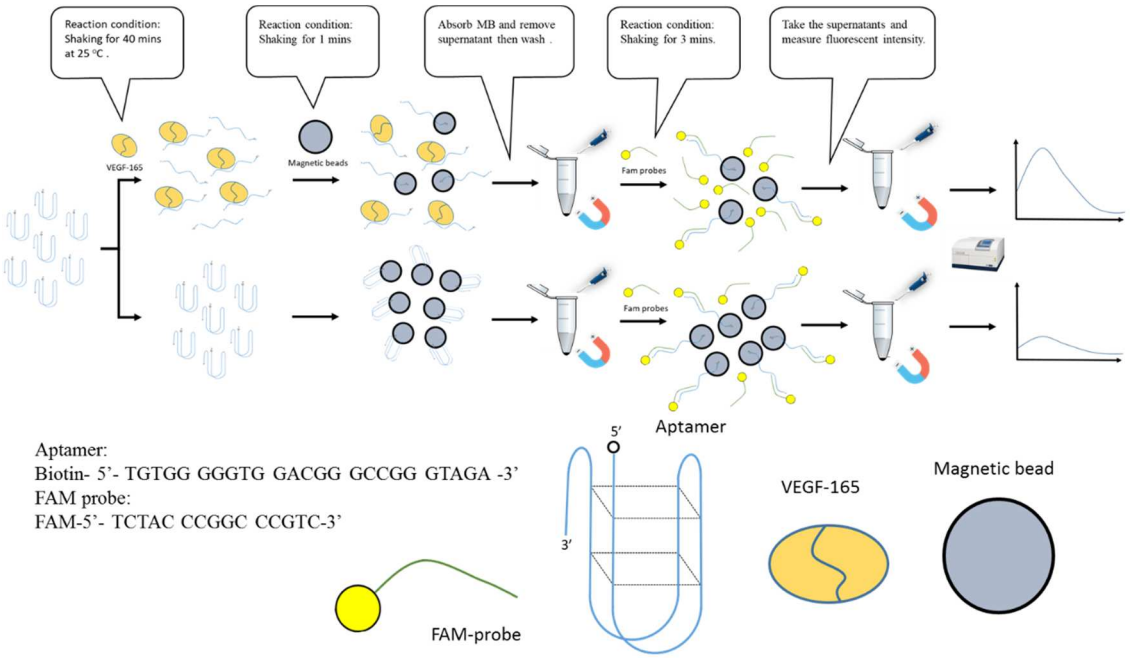

Figure 1. The mechanism of one single tube reaction of aptasensor-based magnetic sensing system for quantitatively sensing VEGF in plasma.

3.2. The method optimization

In this research, the aptasensor-based magnetic sensing system was developed in one single tube for detection of VEGF in plasma. In order to obtain the good sensitivity, specificity and stability under reactions, several parameters were optimized, including the concentration of KCl in the buffer, the buffer pH value (1X TBSE buffer), the concentration of APT, the length of fluorescent probe and the volume of magnetic bead. The data and discussion were as shown in the following.

3.2.1. The concentration of KCl and the buffer pH value

According to the previous researches [47,48], the concentration of KCl would affect the formation of aptamers and the stability of the structure, which in turn determines the affinity of aptamer with VEGF. However, excessively high electrolyte concentration will interact with the residues on the aptamer monomer through the ionic interaction, and electrostatic force acts to form undesired interactions and reduce the affinity of aptamers. Therefore, evaluation of the concentration of KCl is a very important issue in the aptasensor-based sensing system. The different concentrations of KCl, including 30, 40, 50, 60 and 70 μM were investigated under the conditions of the volume of magnetic beads, 10 μL; the concentration of aptamer, 0.1 μM; the concentration of fluorescent probe, 0.01 μM; pH 7 and VEGF concentration of 2 ng/mL for specific detection. The data was as shown in Figure 2A. In the Figure 2A(a), the bar with the black color meant the fluorescence without adding APT in the one single tube reaction. The data presented that the fluorescence without adding APT was stable and unified under various conditions. The bars with the light gray and deep gray color were blank and VEGF samples, respectively. From the data, the fluorescent intensities in the absence of VEGF (F0) and the presence of VEGF (F, 2 ng/mL) were significantly different. Therefore, from Figure 2A(b), the fluorescence rebound ratio under different salt concentrations can be inferred, and in the case of KCl concentration of 50 μM, the aptamer can form the configuration with the best binding effect to VEGF, so the rebound ratio is the highest. Finally, the KCl concentration of 50 μM was selected as the optimal condition for this method.

Preprints (www.preprints.org) | NOT PEER-REVIEWED | Posted: 17 April 2023 doi:10.20944/preprints202304.0451.v1

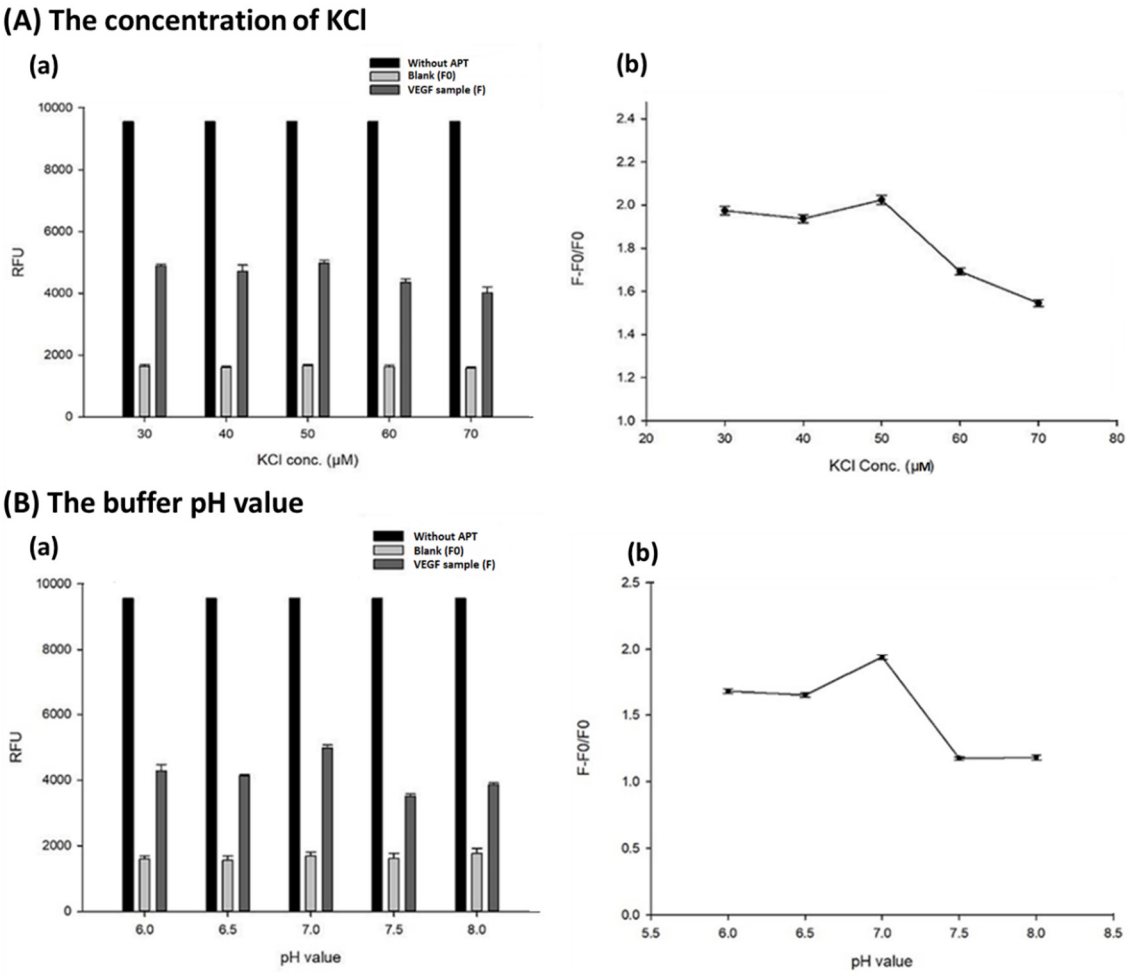

Figure 2. The effect of the concentration of KCl (**A**) and the buffer pH value (**B**) on the aptasensor-based magnetic sensing system. (**a**) The fluorescence under various parameters (n = 3). Experimental conditions are as followed, pH = 7.0, VEGF conc., 2 ng/mL; magnetic beads (MB) volume, 10 μL (4 μg/mL); KCl conc., 50 μM; aptamer (APT) conc., 0.10 μM, fam-labeled probe length, 15 mer (0.01 μM). (**b**) The fluorescence ratios of F-F0/F0 under various conditions (n = 3).

The aptamer itself is a nucleotide sequence. Under the conditions of different pH values, the aptamer will pass through the amide group and the residue on the central carbon of the monomer to form different states of electricity and electricity. Therefore, the different pH values of the buffer would also affect the binding efficiency between the aptamer and the VEGF. In this research, different pH values of the 1X TBSE buffer were evaluated, including pH 6.0, 6.5, 7.0, 7.5 and 8.0. The data was as shown in Figure 2B. Since the aptamer can be regarded as a protein fragment with a complete tertiary structure, it is estimated that when the pH value is 7.4, close to the human body's fluids, it will have a better affinity with VEGF. From the data of Figure 2B(a), the significantly different fluorescent intensities could be observed in the absence of VEGF (F0) and the presence of VEGF (F, 2 ng/mL) under different pH values. In Figure 2B(b), when the pH of the aptamer is neutral (pH = 7.0), the binding effect of aptamer to VEGF is the best, indicating that the aptamer can be bent into a high-affinity configuration in an environment close to the human body, so that the fluorescence rebound ratio reaches the maximum value within the range. Finally, pH 7.0 is selected as the best pH value for this method.

3.2.2. The concentration of APT and the length of fluorescent probe

It is known that APTs can specifically capture the VEGF molecules by forming a structure flexed into a G-quadruplex through forces such as hydrogen bonds between base pairs on the sequence, and

Preprints (www.preprints.org) | NOT PEER-REVIEWED | Posted: 17 April 2023 doi:10.20944/preprints202304.0451.v1

thus, different concentrations of APTs of 0.05, 0.10, 0.15, and 0.20 μM were evaluated. The data was as shown in Figure 3A. From the Figure 3A(a), higher concentrations of aptamers captured on the MB can hybridize more fluorescent probes resulting in the reduce of the fluorescence performance. Therefore, in the presence of VEGF samples, it was observed that the fluorescence decreased at the higher APT concentrations. However, in the blank, the amount of APTs at all different concentrations was much enough to saturate the MB, and there is no significantly fluorescent difference among those. After using the F-F0 / F0 fluorescence rebound (Figure 3A(b), it was found that the maximum value occurred in the utilization of 0.1 μM APT. Therefore, through the evaluation of the ratio of fluorescence rebound, 0.1 μM APT was considered as best binding effect on VEGF in the data representation of aptamer concentrations, and selected as the optimal condition.

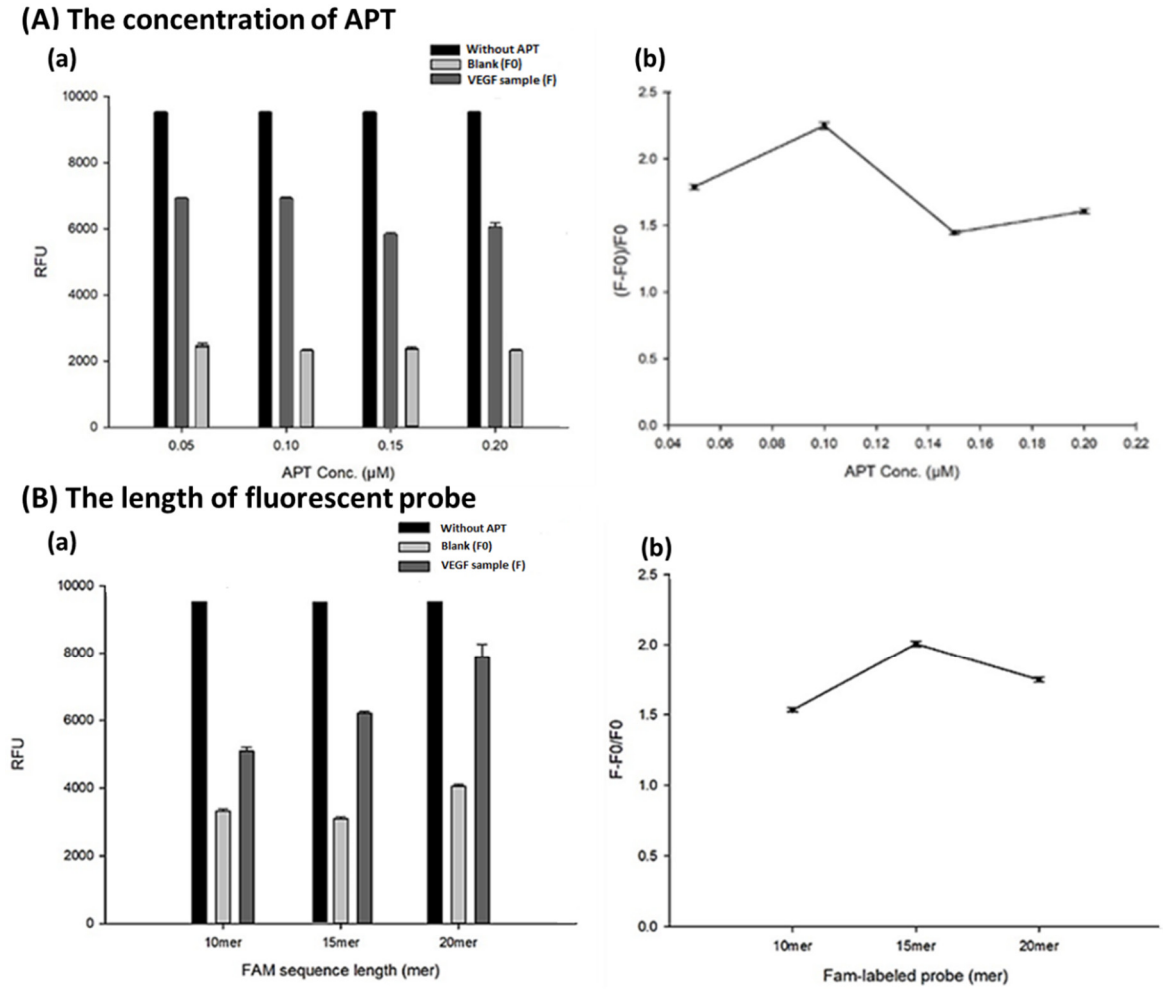

Figure 3. The effect of the concentration of APT (**A**) and the length of fluorescent probe (**B**) on the aptasensor-based magnetic sensing system. (**a**) The fluorescence under various conditions (n = 3). Experimental conditions are as followed, pH = 7.0, VEGF conc., 2 ng/mL; magnetic beads (MB) volume, 10 μL (4 μg/mL); KCl conc., 50 μM; aptamer (APT) conc., 0.10 μM, fam-labeled probe length, 15 mer (0.01 μM). (**b**) The fluorescence ratios of F-F0/F0 under various conditions (n = 3).

Because the length of the fluorescent probes would affect the binding strength with the APT captured on the MB, different length of the fluorescent probes, including 10 mer, 15 mer and 20 mer were evaluated at the concentration of 0.01 μM. The data was as shown in Figure 3B. According to the principle of forming complementary hydrogen bonds between base pairs, it is estimated that when the fluorescent probe sequence is longer, the binding force with the APT on the MB should be higher. The phenome would result in that the lower fluorescence would be observed in the use of

Preprints (www.preprints.org) | NOT PEER-REVIEWED | Posted: 17 April 2023 doi:10.20944/preprints202304.0451.v1

longer fluorescent probes. However, in the Figure 3B(a), the highest fluorescence was taken place in the use of the highest fluorescent probe (20 mer). That was supported the longer probes would more easily form the dimer structures that are difficult to hybridize with the APT, resulting in the higher fluorescence in the longer probes. Through the evaluation of the amount of fluorescent rebound (Figure 3B(b)), the fluorescent probe length of 15 mer had a good binding effect with the APT, and it is regarded as the optimization condition of this method.

3.2.3. The volume of magnetic bead (MBs)

Because the amount of magnetic beads can fully carry the APT and the quantitative effect of the experiment will change due to the amount of MBs, different volume of 5, 10, 15, and 20 μL (4 μg/mL) MBs were investigated. The data was as shown in Figure 4. The main function of magnetic beads is that they can bind with aptamers through covalent bonds and have magnetic force. This magnetic system can help purify the target conjugates, and it can also be easily and quickly completed with the magnets. In Figure 4a with a volume of 5 μL MBs, the amount of MBs is not enough to carry all the aptamers, resulting in more free fluorescent probes and higher fluorescence brightness. In the group of a volume of more than 10 μL, the amount of magnetic beads is enough to carry all the aptamers, so the capture effect for the fluorescent probe has reached saturation, resulting in a similar fluorescence intensity. After referring to the rebound ratio (Figure 4b), the volume of magnetic beads of 10 μL is selected as the best and most economical choice.

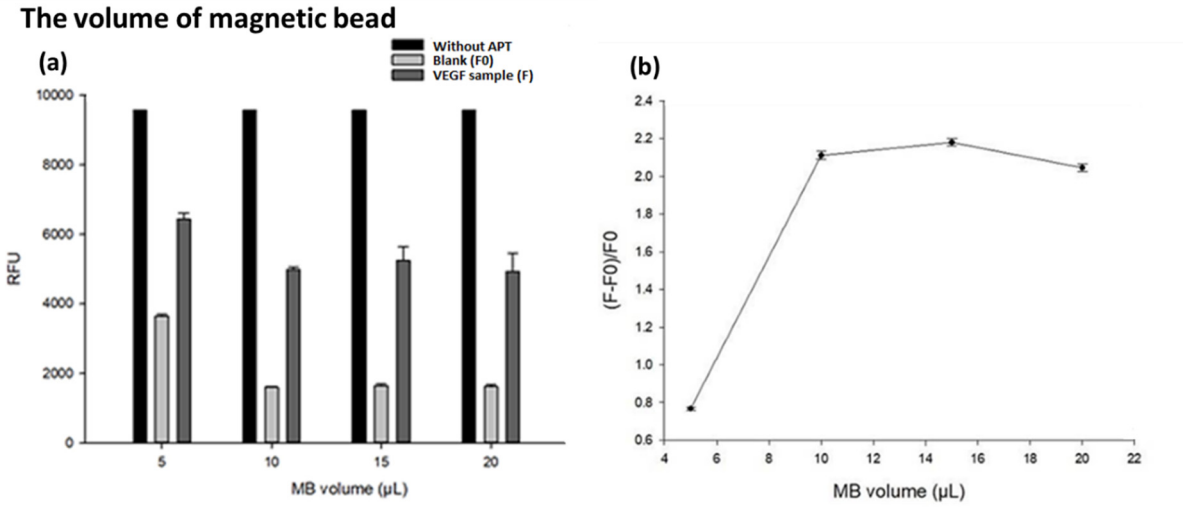

Figure 4. The effect of volume of magnetic bead on the aptasensor-based magnetic sensing system. (**a**) The fluorescence under various conditions (n = 3). Experimental conditions are as followed, pH = 7.0, VEGF conc., 2 ng/mL; magnetic beads (MB) volume, 10 μL (4 μg/mL); KCl conc., 50 μM; aptamer (APT) conc., 0.10 μM, fam-labeled probe length, 15 mer (0.01 μM). (**b**) The fluorescence ratios of F-F0/F0 under various conditions (n = 3).

3.3. The specificity test of the aptasensor system

In order to confirm that this aptasensor-based magnetic sensing system had a highly specific identification ability for VEGF and will not be affected by blood other similar protein effects, thus, several substances commonly found in human body were tested. Whether these common proteins can still maintain a high degree of specificity, the concentration of these common proteins is about 20 times higher than those in human blood. These proteins contained 20 ng/mL bovine serum albumin (BSA), 20 ng/mL albumin (Albumin), 5×10^{-3} U/mL insulin (Insulin) and 2×10^{-3} U/mL mL nitric oxide synthase (NOS) were used as the interfered proteins and VEGF 2 ng/mL as control group to investigate the fluorescence rebound ratio (F-F0/F0). The data was as shown in Figure 5, and it can be confirmed that only the VEGF would have the significant fluorescence rebound ratio. The data

Preprints (www.preprints.org) | NOT PEER-REVIEWED | Posted: 17 April 2023 doi:10.20944/preprints202304.0451.v1

demonstrated this aptasensor-based magnetic sensing system had high specificity when the concentration of other proteins is more than 20 times presented in the human plasma in comparison of the concentration of the test VEGF sample.

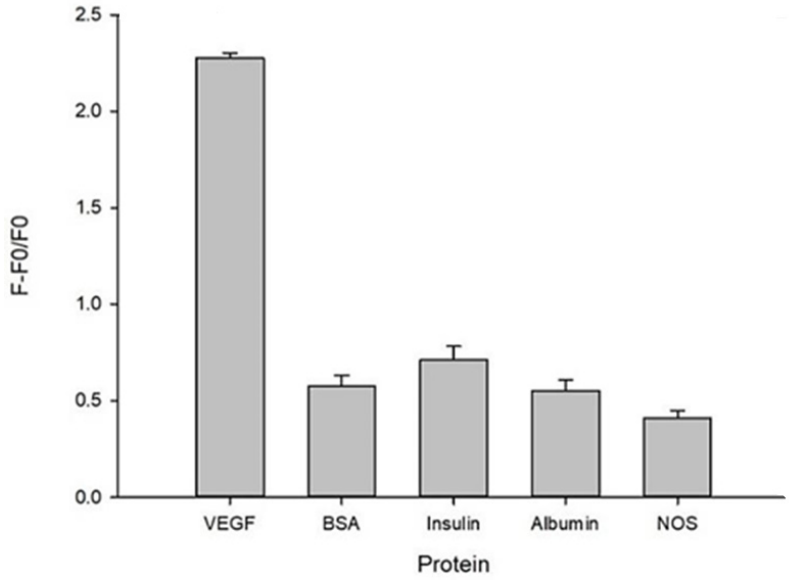

Figure 5. The specificity test of the aptasensor-based magnetic sensing system by using the fluorescence rebound ratio (F-F0/F0) in different kind of regular proteins (n = 3). Experimental conditions are as followed, pH = 7.0, VEGF conc., 2 ng/mL; magnetic beads (MB) volume, 10 μL (4 μg/mL); KCl conc., 50 μM; aptamer (APT) conc., 0.10 μM, fam-labeled probe length, 15 mer (0.01 μM). VEGF conc. = 2.0 ng/mL, BSA conc. = 20 ng/mL, Albumin conc. = 20 ng/mL, insulin conc. = 5×10^{-3} U/mL, NOS = 2×10^{-3} U/mL.

3.4. The application for real plasma samples

After method optimization, the optimal conditions for detection of VEGF were as followed, KCl, 50 μM; pH 7.0; aptamer, 0.1 μM and magnetic beads, 10 μL (4 ng/μL). Under the optimal conditions, the different concentrations of VEGF were spiked at 0.2, 0.5, and 1.5, 2 ng/mL into plasma to establish the calibration curve of real plasma samples. The fluorescent spectra were as shown in the Figure 6A. From the data, it could be obviously found that the fluorescence rebound ratio (F-F0/F0) increased as the VEGF concentration increased. Additionally, without adding the APTs, the fluorescence was the highest one meaning the APTs could be effectively captured by the MBs, and then hybridize with the fluorescent probes to significantly reduce the fluorescence of the supernatant. When the VEGF was spiked into the plasma, the binding of APTs and VEGF would interfere the MBs to capture the APTs, and resulting in the rebound of the fluorescence. By such way, the VEGF in plasma could be easily detected in one single tube reaction. According the fluorescence rebound ratio versus the VEGF concentrations spiked into plasma, the calibration curve could be established and as shown in Figure 6B. The calibration curve possessed a good linearity ($y = 1.0391x + 0.5471$, $r = 0.998$), and the detection limit (LOD) was calculated to be 0.0445 ng/mL according to the formula ($LOD = 3.3 \times \sigma/S$). After establishing the calibration curve, in order to know the recovery of this technique, two concentrations of 0.8 and 1.6 ng/mL VEGF were spiked into the known real plasma sample containing 0.2 ng/mL VEGF, respectively, and using the established regression line to infer the final concentrations. The data was as shown in Table 2. The recoveries of the two spiked concentrations were 116.71% and 102.52%, respectively, indicating that the sensing system can show a good detection effect in real samples.

Preprints (www.preprints.org) | NOT PEER-REVIEWED | Posted: 17 April 2023 doi:10.20944/preprints202304.0451.v1

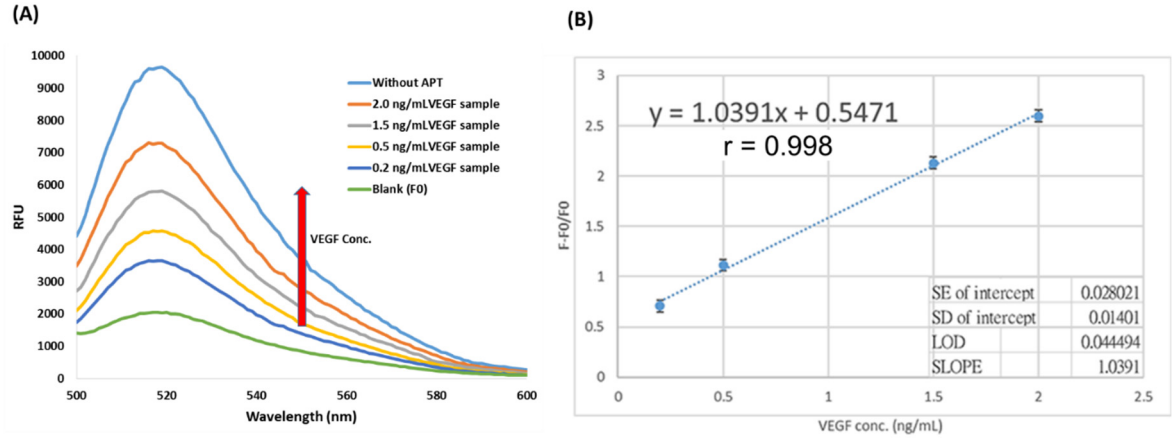

Figure 6. (**A**) The fluorescent spectra of the plasma samples spiked with different VEGF concentrations. (**B**) the calibration curve for quantification of VEGF by using F-F0/F0 vs the concentration of VEGF. Experimental conditions are as followed, pH= 7.0, VEGF conc., 2 ng/mL; magnetic beads (MB) volume, 10 μL (4 μg/mL); KCl conc., 50 μM; aptamer (APT) conc., 0.10 μM, fam-labeled probe length, 15 mer (0.01 μM).

Table 2. Recovery values and precision of VEGF in plasma samples (n=3).

Original VEGF (ng/mL)	Add VEGF (ng/mL)	Concentration Found (ng/mL)	Recovery (%)	RSD (%)
0.20	0.80	1.13±0.03	116.71±2.32	1.9
0.20	1.60	1.84±0.06	102.50±3.41	3.3

4. Conclusions

In cancer treatment, the development of drugs has encountered a bottleneck, and clinical treatment policy has begun to shift to the biomarker of the proliferation of solid tumor cells, vascular endothelial cell growth factor (VEGF). In the review of meta-analysis in 2007, it was mentioned that the blood concentration of VEGF in breast cancer patients was about ten times that of normal human blood [30], so the value of the blood concentration of VEGF can not only be used to help the diagnosis of cancer types but also monitor the progress of tumor cells in treatment throughout the course of the disease. Therefore, rapid and accurate detection of VEGF blood levels plays a very important role in cancer treatment. However, most of the current VEGF detection methods require professional detection instruments and experienced operators, and the detection process takes a relatively long time and is not universal [49]. Therefore, in this study, a simple, rapid and easy-to-use quantitative detection strategy, one single tube reaction of aptasensor-based magnetic sensing system has been successfully established for detection of VEGF in plasma. This VEFG detection strategy developed by combining the design and optimized conditions of this study has been proved to be effective and specific in identifying VEGF in plasma, and all detection operations can be completed in as little as 50 minutes, which can achieve simple, fast, low cost and high sensitivity characteristics. This strategy provided a simple, sensitive and selective biosensing platform for detection of serum VEGF, and it was expected that this detection technique can be promoted to more clinical applications.

Author Contributions: Hwang-Shang Kou: Methodology, Validation, Investigation, Data Curation; Shao-Tsung Lo: Validation, Investigation, Data Curation; Chun-Chi Wang: Methodology, Validation, Investigation, Data Curation, Writing—Original Draft, Review & editing, Revision.

Institutional Review Board Statement: Not applicable.

Informed Consent Statement: Not applicable.

Data Availability Statement: Data reported in the study are available from the corresponding author on reasonable request.

Acknowledgments: We extend our deep and sincere thanks to volunteers who kindly contributed samples that were crucial to this study. We gratefully acknowledge the support of the Ministry of Science and Technology of Taiwan (MOST 110-2113-M-037-013) for the funding of this work and the help of Kaohsiung Medical University Chung-Ho Memorial Hospital, Kaohsiung, Taiwan.

Conflicts of Interest: The authors declare no conflict of intere

References

1. Haukanes, B.-I.; Kvam, C. Application of magnetic beads in bioassays. *Biotechnology* **1993**, 11, 60-63.
2. Wilson, R. Preparation of single-stranded DNA from PCR products with streptavidin magnetic beads. *Nucleic Acid Ther.* **2011**, 21, 437-440.
3. Tu, S.I.; Uknalis, J.; Irwin, P.; Yu, L.S. The use of streptavidin coated magnetic beads for detecting pathogenic bacteria by light addressable potentiometric sensor (LAPS). *J. rapid methods autom. micribiol.* **2000**, 8, 95-109.
4. Bruno, J.G.; Kiel, J.L. Use of magnetic beads in selection and detection of biotoxin aptamers by electrochemiluminescence and enzymatic methods. *BioTechniques* **2002**, 32, 178-183.
5. Zhang, H.; Yu, D.; Zhao, Y.; Fan, A. Turn-on chemiluminescent sensing platform for label-free protease detection using streptavidin-modified magnetic beads. *Biosens. Bioelectron.* **2014**, 61, 45-50.
6. Ohara, R.; Ohara, O. A new solid-phase chemical DNA sequencing method which uses streptavidin-coated magnetic beads. *DNA Research* **1995**, 2, 123-128.
7. Wang, C.; Yang, G.; Luo, Z.; Ding, H. In vitro selection of high-affinity DNA aptamers for streptavidin. *Acta Biochim. Biophys. Sin.* **2009**, 41, 335-340.
8. BelBruno, J.J. Molecularly Imprinted Polymers. *Chem. Rev.* **2019**, 119, 1, 94–119.
9. Toh, S.Y.; Citartan, M.; Gopinath, S.C.; Tang, T.-H. Aptamers as a replacement for antibodies in enzyme-linked immunosorbent assay. *Biosens. Bioelectron.* **2015**, 64, 392-403.
10. Chen, A.; Yang, S. Replacing antibodies with aptamers in lateral flow immunoassay. *Biosens. Bioelectron.* **2015**, 71, 230-242.
11. Nezlin, R. Use of aptamers in immunoassays. *Mol. Immunol.* **2016**, 70, 149-154.
12. Dunn, M.R.; Jimenez, R.M.; Chaput, J.C. Analysis of aptamer discovery and technology. *Nat. Rev. Chem.* **2017**, 1, 1-16.
13. Koide, H.; Yoshimatsu, K.; Hoshino, Y.; Lee, S.-H.; Okajima, A.; Ariizumi, S.; Narita, Y.; Yonamine, Y.; Weisman, A.C.; Nishimura, Y. A polymer nanoparticle with engineered affinity for a vascular endothelial growth factor (VEGF 165). *Nat. Chem.* **2017**, 9, 715-722.
14. Song, S.; Wang, L.; Li, J.; Fan, C.; Zhao, J. Aptamer-based biosensors. *TrAC, Trends Anal. Chem.* **2008**, 27, 108-117.
15. Iliuk, A.B.; Hu, L.; Tao, W.A. Aptamer in bioanalytical applications. *Anal. Chem.* **2011**, 83, 4440-4452.
16. Sullivan, R.; Adams, M.C.; Naik, R.R.; Milam, V.T. Analyzing secondary structure patterns in DNA aptamers identified via CompELS. *Molecules* **2019**, 24, 1572.
17. Afanasyeva, A.; Nagao, C.; Mizuguchi, K. Prediction of the secondary structure of short DNA. *Biophysics and physicobiology* **2019**, 16, 287-294.
18. Nezlin, R. Use of aptamers in immunoassays. *Mol. Immunol.* **2016,** 70, 149-154.
19. Huang, J.; Chen, X.; Fu, X.; Li, Z.; Huang, Y.; Liang, C. Advances in aptamer-based biomarker discovery. *Front. Cell Dev. Biol.* **2021,** 9, 571.
20. Yang, M.; Jiang, G.; Li, W.; Qiu, K.; Zhang, M.; Carter, C.M.; Al-Quran, S.Z.; Li, Y. Developing aptamer probes for acute myelogenous leukemia detection and surface protein biomarker discovery. *J. Hematol. Oncol.* **2014**, 7, 1-14.
21. Shibuya, M. Vascular Endothelial Growth Factor (VEGF) and Its Receptor (VEGFR) Signaling in Angiogenesis. *Genes Cancer* **2011**, 2, 1097–1105.
22. Mansoori, B.; Mohammadi, A.; Davudian, S.; Shirjang, S.; Baradaran, B. The different mechanisms of cancer drug resistance: a brief review. *Adv. Pharm. Bull.* **2017**, 7, 339.
23. Gottesman, M.M. Mechanisms of cancer drug resistance. *Annu. Rev. Med.* **2002**, 53, 615-627.
24. Housman, G.; Byler, S.; Heerboth, S.; Lapinska, K.; Longacre, M.; Snyder, N.; Sarkar, S. Drug resistance in cancer: an overview. *Cancers* **2014**, 6, 1769-1792.
25. Shibuya, M. Structure and function of VEGF/VEGF-receptor system involved in angiogenesis. *Cell Struct. Funct.* **2001**, 26, 25-35.
26. Li, T.; Kang, G.; Wang, T.; Huang, H. Tumor angiogenesis and anti-angiogenic gene therapy for cancer. *Oncol. Lett.* **2018**, 16, 687-702.
27. Carmeliet, P.; Jain, R.K. Angiogenesis in cancer and other diseases. *Nature* **2000**, 407, 249-257.
28. Tamura, M.; Ohta, Y.; Kajita, T.; Kimura, K.; Go, T.; Oda, M.; Nakamura, H.; Watanabe, G. Plasma VEGF concentration can predict the tumor angiogenic capacity in non-small cell lung cancer. *Oncol. Rep.* **2001**, 8, 1097-1102.

29. Kopeć, M.; Abramczyk, H. Angiogenesis-a crucial step in breast cancer growth, progression and dissemination by Raman imaging. *Spectrochim. Acta A Mol. Biomol. Spectrosc.* **2018**, 198, 338-345.
30. Kut, C.; Mac Gabhann, F.; Popel, A. Where is VEGF in the body? A meta-analysis of VEGF distribution in cancer. *Br. J. Cancer* **2007**, 97, 978-985.
31. Parveen, A.; Subedi, L.; Kim, H.W.; Khan, Z.; Zahra, Z.; Farooqi, M.Q.; Kim, S.Y. Phytochemicals targeting VEGF and VEGF-related multifactors as anticancer therapy. *J. Clin. Med.* **2019**, 8, 350.
32. Zhang, M.; Liu, J.; Liu, G.; Xing, Z.; Jia, Z.; Li, J.; Wang, W.; Wang, J.; Qin, L.; Wang, X. Anti-vascular endothelial growth factor therapy in breast cancer: Molecular pathway, potential targets, and current treatment strategies. *Cancer Lett.* **2021**, 520, 422-433.
33. Hsu, M.-Y.; Yang, C.-Y.; Hsu, W.-H.; Lin, K.-H.; Wang, C.-Y.; Shen, Y.-C.; Chen, Y.-C.; Chau, S.-F.; Tsai, H.-Y.; Cheng, C.-M. Monitoring the VEGF level in aqueous humor of patients with ophthalmologically relevant diseases via ultrahigh sensitive paper-based ELISA. *Biomaterials* **2014**, 35, 3729-3735.
34. Mineta, H.; Miura, K.; Ogino, T.; Takebayashi, S.; Misawa, K.; Ueda, Y.; Suzuki, I.; Dictor, M.; Borg, Å.; Wennerberg, J. Prognostic value of vascular endothelial growth factor (VEGF) in head and neck squamous cell carcinomas. *Br. J. Cancer* **2000**, 83, 775-781.
35. Vasala, A.; Nair, H.; Rao, T.S.; Murthy, S.S.; Tagore, R.; Ahmed, F. Role of angiogenesis in colorectal carcinomas using VEGF and BCl2: an IHC study. *Ann. Diagn. Pathol.* **2017**, 31, 41-44.
36. Anthony, F.; Evans, P.; Wheeler, T.; Wood, P. Variation in detection of VEGF in maternal serum by immunoassay and the possible influence of binding proteins. *Ann. Clin. Biochem.* **1997**, 34, 276-280.
37. Sumner, G.; Georgaros, C.; Rafique, A.; DiCioccio, T.; Martin, J.; Papadopoulos, N.; Daly, T.; Torri, A. Anti-VEGF drug interference with VEGF quantitation in the R&D systems human quantikine VEGF ELISA kit. *Bioanalysis* **2019**, 11, 381-392.
38. Lin, X.; Leung, K.-H.; Lin, L.; Lin, L.; Lin, S.; Leung, C.-H.; Ma, D.-L.; Lin, J.-M. Determination of cell metabolite VEGF165 and dynamic analysis of protein–DNA interactions by combination of microfluidic technique and luminescent switch-on probe. *Biosens. Bioelectron.* **2016**, 79, 41-47.
39. Pasquardini, L.; Pancheri, L.; Potrich, C.; Ferri, A.; Piemonte, C.; Lunelli, L.; Napione, L.; Comunanza, V.; Alvaro, M.; Vanzetti, L. SPAD aptasensor for the detection of circulating protein biomarkers. *Biosens. Bioelectron.* **2015**, 68, 500-507.
40. Li, J.; Sun, K.; Chen, Z.; Shi, J.; Zhou, D.; Xie, G. A fluorescence biosensor for VEGF detection based on DNA assembly structure switching and isothermal amplification. *Biosens. Bioelectron.* **2017**, 89, 964-969.
41. Chattaraj, R.; Mohan, P.; Livingston, C.M.; Besmer, J.D.; Kumar, K.; Goodwin, A.P. Mutually-reactive, fluorogenic hydrocyanine/quinone reporter pairs for in-solution biosensing via nanodroplet association. *ACS Appl. Mater. Interfaces* **2016**, 8, 802-808.
42. Zhang, H.; Peng, L.; Li, M.; Ma, J.; Qi, S.; Chen, H.; Zhou, L.; Chen, X. A label-free colorimetric biosensor for sensitive detection of vascular endothelial growth factor-165. *Analyst* **2017**, 142, 2419-2425.
43. Li, Y.; Lee, H.J.; Corn, R.M. Detection of protein biomarkers using RNA aptamer microarrays and enzymatically amplified surface plasmon resonance imaging. *Anal. Chem.* **2007**, 79, 1082-1088.
44. Cennamo, N.; Pesavento, M.; Lunelli, L.; Vanzetti, L.; Pederzolli, C.; Zeni, L.; Pasquardini, L. An easy way to realize SPR aptasensor: A multimode plastic optical fiber platform for cancer biomarkers detection. *Talanta* **2015**, 140, 88-95.
45. Chen, H.; Hou, Y.; Qi, F.; Zhang, J.; Koh, K.; Shen, Z.; Li, G. Detection of vascular endothelial growth factor based on rolling circle amplification as a means of signal enhancement in surface plasmon resonance. *Biosens. Bioelectron.* **2014**, 61, 83-87.
46. Lee, J.-H.; Canny, M.D.; De Erkenez, A.; Krilleke, D.; Ng, Y.-S.; Shima, D.T.; Pardi, A.; Jucker, F. A therapeutic aptamer inhibits angiogenesis by specifically targeting the heparin binding domain of VEGF165. *Proc. Natl. Acad. Sci. U.S.A.* **2005**, 102, 18902-18907.
47. Cao, J.; Zhao, X.P.; Younis, M.R.; Li, Z.Q.; Xia, X.H.; Wang, C. Ultrasensitive Capture, Detection, and Release of Circulating Tumor Cells Using a Nanochannel-Ion Channel Hybrid Coupled with Electrochemical Detection Technique. *Anal Chem.* **2017**, 89, 10957-10964.
48. Cai, W.; Fan, Y.; Jiang, Z.; Yao, J. A highly sensitive and selective resonance scattering spectral assay for potassium ion based on aptamer and nanosilver aggregation reactions. *Talanta* **2010**, 81, 1810-1815.
49. Dehghani, S.; Nosrati, R.; Yousefi, M.; Nezami, A.; Soltani, F.; Taghdisi, S.M., Abnous, K.; Alibolandi, M.; Ramezani, M. Aptamer-based biosensors and nanosensors for the detection of vascular endothelial growth factor (VEGF): A review. *Biosens. Bioelectron.* **2018**, 110, 23-37.